

# Coarse Geometry acquisition of welding parts using a novel cheap depth sensor

Thorsten Gecks, University of Bayreuth, Lehrstuhl für Angewandte Informatik III, 95440 Bayreuth, Germany  
Christopher Müller, Blackbird Robotersysteme GmbH, Erfurter Strasse 5, 85386 Eching, Germany  
Dominik Henrich, University of Bayreuth, Lehrstuhl für Angewandte Informatik III, 95440 Bayreuth, Germany  
Wolfgang Vogl, Blackbird Robotersysteme GmbH, Erfurter Strasse 5, 85386 Eching, Germany

## Abstract

We present a human-robot-cooperation welding system, consisting of several phases including a coarse acquisition of the work piece geometry, interactive fine-scanning of welding seam regions and automated optimizing path planning after task specification by the user. The coarse geometry acquisition component is explained in detail showing the feasible application of a novel and cheap 3D-Sensor (MS KINECT) in this domain. The evaluation shows promising and sufficient results for planning the acquisition of high-resolution fine scans using a standard laser scanner and the use of an automated path planning component. The path planning is based on a bidirectional RRT planner followed by a path optimization. The system thus enables the human coworker to specify a welding task for unknown geometries fast to the machine and relieves him from the tedious robot movement planning during the actual welding phase.

## 1 Introduction

Production in the high-wage countries of the European Union can only remain competitive by an increase of productivity fostered by automation while keeping the quality and accuracy of produced goods. A key factor for this will be the extension of robotic automation from automotive mass production to a broad use in the general industry, especially to the area of small or even single lot-size production. With 29% out of the 1 million worldwide stocks, welding is the central domain of robot-

based factory automation [3].

Considering today's robot automation with respect to small lot-size welding applications, several central limitations can be observed. Unlike the completely digital engineering process in the automotive industry, process chains in the general industry often do not provide *CAD models* both suited and precise enough for offline programming. Even with CAD models available, the process of finding a suitable motion sequence (collision-free, within the process boundaries, smooth and even motion, optimized execution time) is a highly time consuming task. Especially as most welding systems use exter-

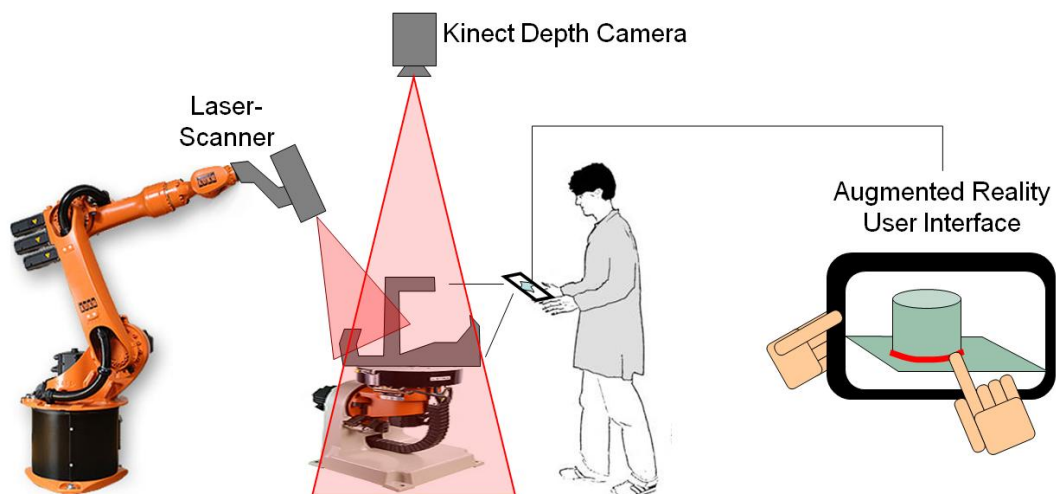


**Figure 1** Hardware setup with a KUKA KR16-2 robot on the left with a (symbolic) laser scanner affixed to the TCP, a statically mounted KINECT camera at the top (work cell structures are not shown) and a turn-tilt-table with a symbolic work-piece placed on it in the middle. The augmented reality scenario is part of the project, but not discussed in this paper.

nal positioning axes, such that the programmer has to deal with 8 or 9 motion axes and additional degrees-of-freedom stemming from the process [Munzert09]. Today's offline programming systems just transfer the trial-and-error approach of teach-in programming to the virtual world but do provide no or only little functionality for *automated motion planning*. The experience from existing human-robot co-welding systems shows that teach-in by *demonstration through force-guided interfaces* is too slow and not accurate enough [7,8], and provides only a low-level task specification interface. Also, the force-guided robot may impose peculiar constraints do to movement limitations of the kinematic chain.

Therefore today, in the face of small or even single lot-size production, the efforts required for robot programming outweigh the economic benefits of automating the welding task. In the outcome today there is an unbridgeable gap between fully-automated but complex to handle systems on the one hand side and a pure manual execution of welding tasks on the other hand.

The EU-funded project COWBOI aims at developing a small lot-size human-robot cooperative welding system. The system shall enable welding with an interactive, intuitive, fast and accurate task specification by the user. One of the major aspects constitutes the visual communication interface between the human and the robot system enabling fast task communication. Another aspect is the interactive geometry acquisition and weld seam specification through visual sensors increasing efficiency in task communication. An additional aspect comparing to existing approaches is the increase in robot system autonomy in both task suggestions as well as autonomous task-based movement planning.

The system consists of four major components: coarse geometry acquisition, interactive fine geometry acquisition, task description by the user and automated path planning.

The coarse geometry of the unknown work piece, of clamping devices and other obstacles in the scene needs to be acquired to facilitate collision-free autonomous path planning. Whilst there are scenarios where the welding of a seam requires virtually no collision checking and can be proposed by the user easily, in more complex arrangements the extents of the welding torch, the robot and the work piece need to be considered including motion constraints of the robot. This could be far too difficult or at least an error-prone time-consuming task for the human operator, so an automatic planning component is required and therefore collision detection based on a coarse model. The acquisition system is based on a novel, cheap depth sensor (MS KINECT). The acquisition process and the results are presented in Section 2 below.

Based on the coarse model acquired in the first step, the user may specify regions of interest, which are subsequently fine-scanned by the robot using a laser scanner mounted on the robot flange. This way an accurate model of certain parts of the work piece is acquired to facilitate the welding. This process is described in Section 3.

With the digital model of the work piece loaded into a virtual simulation environment, the user can describe and further specify task and tool parameters by means of simple CAD-based input metaphors. This process step has been described in [6].

The automated process planning involves finding a short, collision-free sequence for the single operations of the welding tasks through a suitable adaptation of heuristics. This resembles in principle a rural post-man problem (shortest edge tour through a graph with a subset of mandatory edges) as each seam may – in order to minimise thermal deformation – be assigned restrictions in terms of welding direction and subsets of the seams may be grouped in an invariable sequence. The details are described in Section 4.

## 2 Coarse geometry acquisition

In this section we give detail about how the coarse geometry of a work piece (Figure 2) is acquired to facilitate the specification of fine scan motions using a triangulation laser scanner and the planning of the actual welding motion.

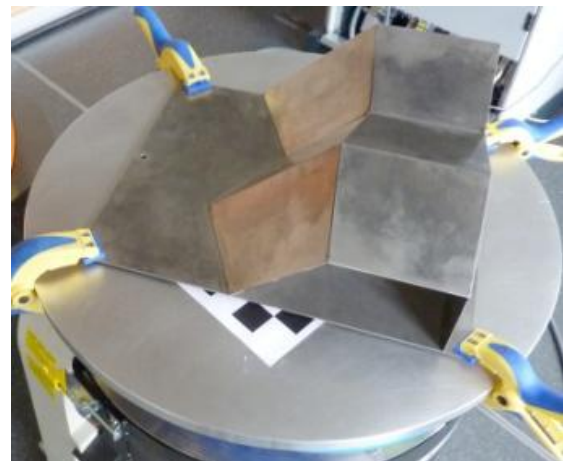


**Figure 2** Steel welding part affixed to the top of the turn-tilt-table.

The laser scanner operates in close distance to the object at an average of 200 mm to the object surface with a detection range of about 100mm. The accuracy of the sensor that acquires the coarse surface should thus be at least below this value to enable a single-pass fine scan movement for a specific region of interest.

In late 2010, a cheap (ca. 100 €) depth sensor was introduced by Microsoft Corporation, initially for

their gaming console product. Shortly after product release there have been solutions for acquisition of sensor data on a standard workstation PC. Since the theoretical accuracy of the product is well below the accuracy necessary for this application, the sensor was employed for coarse geometry acquisition.

Approaches exist to acquire geometric information of an object via visual/stereo hull reconstruction or by using multiple depth sensors and fusing these [1, 4]. Here we employ a single MS KINECT Sensor in combination with a turn-tilt-table to reconstruct a rigid metal work piece (see Figure 2) with reflective surface from several viewpoints.

By moving the turn-tilt-table and acquiring images from a static KINECT camera, which is calibrated w.r.t the robot coordinate system, a series of different viewpoints are generated randomly/evenly to cover a virtual half sphere defined in relation to the table-top coordinate system to sample all possible surface normals of the object from an almost perpendicular viewpoint. This is best for detection as at oblique viewing angles the active signal from the sensor (a collection of IR-laser-beams forming pseudo-random dots on surfaces) might get reflected away from the detecting camera in the sensor by the metal surface leading to misdetections.

The acquired space in the table-top coordinate system is a cube of 800 mm side length subdivided into a grid representation (voxel space) with 128 subdivisions in each of the coordinate directions. Each voxel center is transformed into the camera coordinate system to compare against the depth measurements of the camera to determine the occupancy of this voxel. Afterwards, the occupancy grid is triangulated using the *Marching Cubes* algorithm [9].

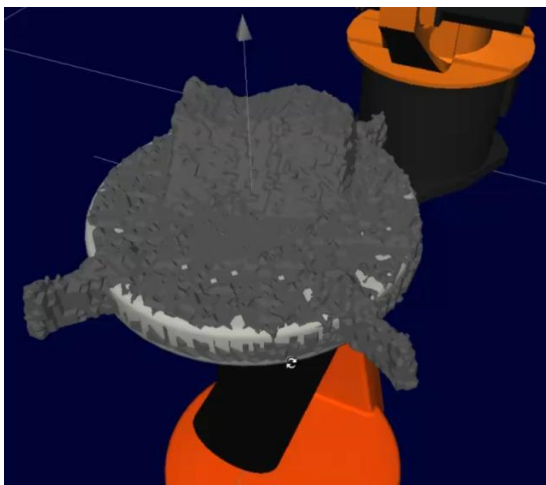


**Figure 3** The coarse 3D model acquired from fusing the sensor data of a total number of 12x10 images. The 3D-model is loaded into a simulation of the work space comprising known parts such as the robot and the turn-tilt-table, which are modeled exactly from CAD data.

The results from this process using 12 different views of the prototype steel part (Figure 2) are shown in Figure 3. The model obtained from the sensor data processing includes parts of the turn-tilt-table and fixtures. The flat part of the object does not separate clearly from the turn-tilt-table, thus indicating at a lower resolution limit of ca 10 mm at a distance of 1500-2000 mm.

The occupancy of a voxel is determined by counting three values: the *occupied count* (when the sensor determines the voxel to be behind the first surface it detects), the *free count* (the opposite of the former) and the count of all misdetections. A fourth category is not explicitly measured, it happens if a voxel is outside of the viewing volumes of the camera, which is a pyramid frustum with minimum and maximum detection range.

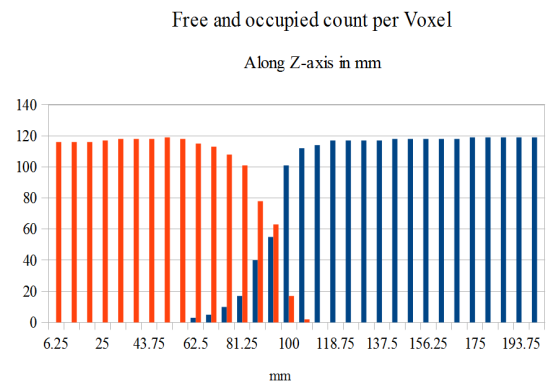


**Figure 4** Diagram showing the free and occupied counts per voxel of the work piece detected by the sensor on a set of voxels along the Z-axis in the middle of the table (perpendicular to the table plane) over all measurements taken. These numbers do not all add up to the total sum of 120 measurements as there has been a number of misdetections by the sensor occasionally.

The free and occupied counts for each voxel along the Z-axis in the center of the cube (in the XY-plane) are shown in Figure 4. The Z-axis is perpendicular to the table plane and also depicted in Figure 3. In this example the sensor detects a voxel both occupied and free in a number of images. It happens in a range from ~ 60 mm to ~ 105 mm, indicating the sensor noise.

The sensor is also incapable of measuring the edges of objects accurately due to the measurement principle, which boils down to the correspondence detection of a collection of neighboring pseudo-random points that are formed by the IR beams of the sensor. In the vicinity of edges only a very noisy signal or even no signal can be acquired. As a consequence, in the reconstruction using the free and occupied counts mentioned above, edges tend to get round as voxels that are in close proximity to the edge are not detected.

Also, depending on the reflectivity and geometry of the surface the detection quality may vary largely and would need to be determined for any material. In Figure 9, an example for a highly problematic material is shown, leading to much misdetection.



**Figure 5** Example of a crinkled aluminum foil (ca. 15 x 20 mm) leading to sensor misdetections in a distance of ca. 1700 mm.

Nevertheless, regarding the purposes of this application and the detection properties of the metallic surface used the overall resolution and noise is sufficient to facilitate the collision-free path planning for the actual welding phase and supply the data to enable the specification of fine scanning regions.

### 3 Fine geometry acquisition

In this section we give an outline of how the user can specify regions on the work piece that require fine scans in order to define the final, accurate position of the welding seams. The user specifies these by means of linear movement specification in a simulation environment (see Figure 6) and based on the coarse sensor data acquired in the previous step, which is visualized to him in the simulation.

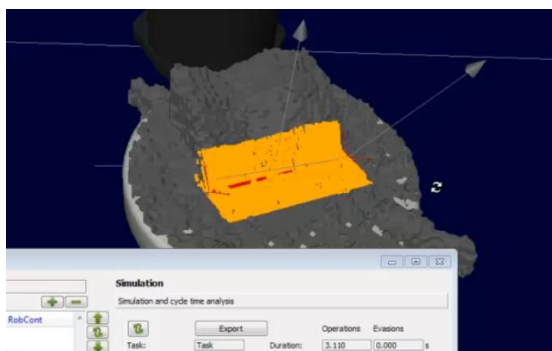


**Figure 6** Specification of the scanned part of the work piece in the simulation user interface. The yellow part on the work piece is marked for scanning.

A laser scanner mounted to the robot flange and registered with the robot coordinate system is then used to acquire the necessary fine scan data (see Figure 7).

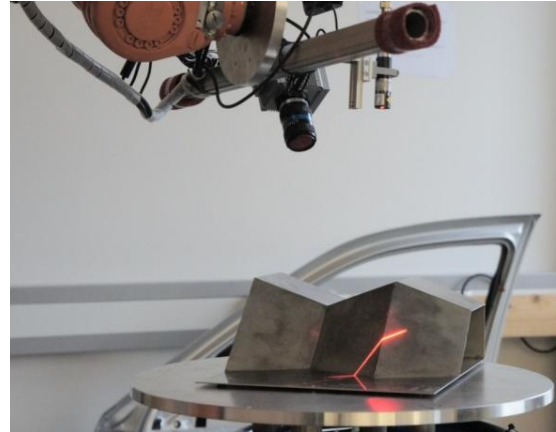


**Figure 7** Laser scanner (triangulation principle) mounted to the flange of the robot.

The resolution of the laser scanner is 0.1 mm and thus allows for precise specification of the welding seams in user interface, similar to the specification of fine scanning motions (see Figure 8).

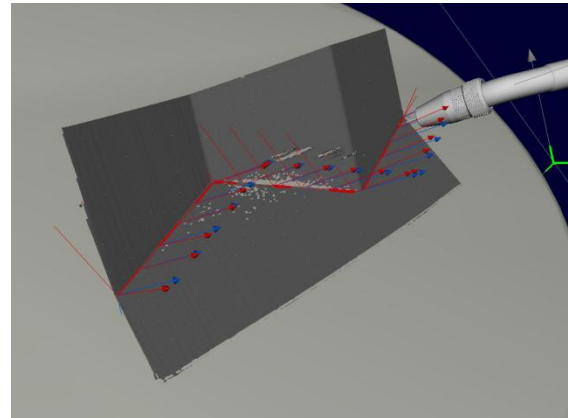


**Figure 8** Specification of a (striped) welding seam in the simulation environment based on the fine scan data acquired by the laser scanner. The coarse model data is not shown.

### 4 Automated path planning

In this section we present the path planning based on the exact specification of the welding seams and using the coarse model for collision detection.

Automated path planning within the welding phase may be distinguished into two phases: on the one hand the planning during the welding of a seam within its given range of process parameters and on the other hand the planning between multiple discontinuous seams. Based on the coarse scan geometry data and the corresponding CAD model of the chosen robot a fast collision detection using the collision library PQP [2] can be established (see Figure 9).

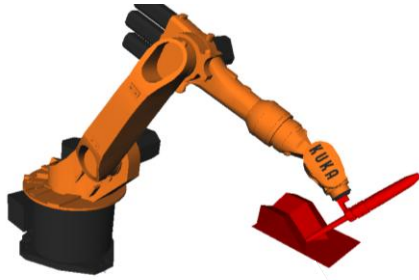


**Figure 9** Visualization of a collision between scan data model and cad model of the welding tool within the 3D scene of the RobotMotionCenter.

For both cases a bidirectional single query path planner based on rapidly exploring random trees (RRT) has been implemented [5]. However, depending on user defined process parameters (i.e. inclination angles) the configuration space is strictly restricted for the first case. For this reason and because of the fixed TCP position along the welding seam, using an inverse kinematics sampling strategy within the workspace of the robot is the fastest way to go. For each welding seam fixed start and end configurations are considered. Based on the bidirectional RRT-Connect algorithm configurations within the welding seam are sampled if not already collision-free. However, in order to make sure the TCP trajectory stays on the welding seam all the time, the local planner is testing the direct Cartesian connection between two configurations in the workspace of the robot for a collision. If a sample is in collision, an adaption within the given process parameters is performed in order to get a collision-free sample. Afterwards the resulting TCP welding trajectory can be optimized using a standard path pruning algorithm. Because of the random sampling within the process parameters of the welding seam the resulting path can be arbitrarily bad in terms of smoothness of the robot tool trajectory given by the center of mass of the tool (see Figure 10).

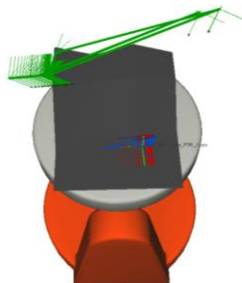


**Figure 10** Collision-free planning of a welding seam using an RRT-Connect planner based on workspace sampling. The green trajectory (green) is given by the center of mass of the tool.

In order to minimize the problem of the changing orientation along the path, the distance metric has to take the angular distance into account. In addition

to the use of an appropriate metric, the orientations of adjacent configurations may be adjusted to each other within their respective process parameters in a way, that their direct Cartesian connection still stays collision-free (see Figure 11).

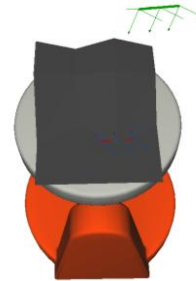


**Figure 11** Collision-free planning of a welding seam using an RRT-Connect planner based on workspace sampling. The tool trajectory was optimized by adjusting the orientations of adjacent configurations followed by a path pruning step.

A more simple approach is based on bisection. Each time a collision is detected, the algorithm creates a new sample point on the welding seam and adjusts its orientation until a collision-free configuration within the given process parameters is found. Recursively a collision-free welding seam is created. Thereby the adjustment of the orientations is based on the orientation of their respective closest neighbor sample (see

Figure 12

**Figure 12).**

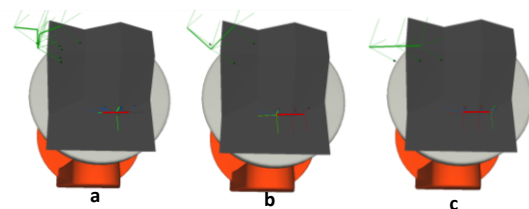


**Figure 12** (a) Collision-free planning of a welding seam by bisecting the seam without optimization. (b) Optimized using path pruning. (c) Optimized by adjusting the orientations of adjacent configurations.

Based on the test scenario with an 75mm welding seam and the complete fine scan data, the average data of the computation time, the number of generated collision-free elements on the seam as well as the length of the tool trajectory were computed doing 10 runs on a Core i5 2x2,4 GHz with 4GB of RAM (see Figure 13) .

	Elements	Time (ms)	Tool trajectory (mm)
<b>RRT</b>	40,2	26418,4	1372,9649
<b>Bisect</b>	4	7315	131,236

**Figure 13** Average computation data without optimization of RRT and Bisect planner based on 10 test runs.

For this simple test case, the approach based on bisection of the welding seam leads to faster and better results. In order to provide a fast and efficient way to solve the rural postman problem of the latter case, a heuristic algorithm based on a k-Opt algorithm is used. Starting with any given tour, this algorithm successively tries to enhance this tour by replacing random edges [6] (see Figure 14).

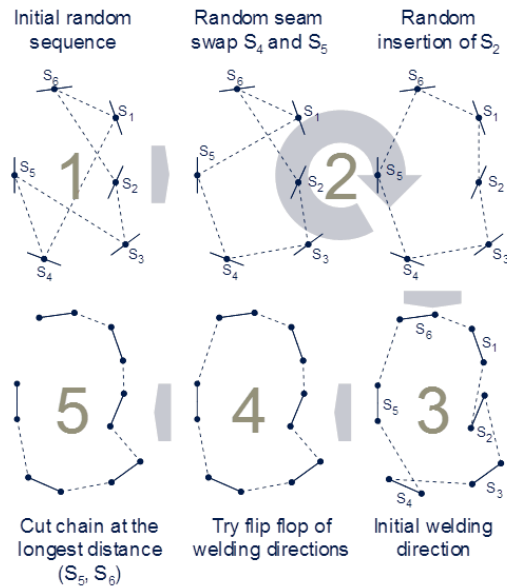


**Figure 14** Methodology of the adapted k-Opt heuristic to compute a shortest welding motion [6].

Considering the small sizes of the seams in relation to the transfer movements the problem can be approximated by a symmetric traveling salesman problem in a first step. Using the geometric center of each seam, the implemented k-Opt algorithm is capable of finding a shortest sequence by deleting k random edges within the Hamilton cycle and re-assembling the remaining ones back into a single tour. Based on this shortest tour each seam is modeled by two points - starting and end point - in order to factor the geometric size of the seams into account. This results in an extended Hamilton cycle. Randomly switching the welding directions of the seams leads to even shorter sequences. After a defined number of iterations, a shortest tour can be extracted by cutting the resulting tour at the longest transfer movement, defining starting and end point of the welding motion.

## 5 Conclusion

In this paper we present the first use of the KINECT RGB-D sensor to acquire geometric models of welding parts to supply these in lack of CAD-models in a semi-automatic interactive welding process for small-lot-size manufacturing. The acquisition results show a good performance of

the sensor even with reflective surfaces suitable for collision testing in sub-sequent planning of fine-scanning steps (using a standard laser scanner). Borderline detection cases at certain viewing angles can be alleviated fusing a number of different viewpoints using a turn-tilt-table. In our future work, we will focus on the problem of automatically planning a collision-free robot motion as optimal as possible in terms of sequence, total path length and collision within the welding seams considering multiple start and goal configurations for each welding seam.

## 6 Literature

- [1] Fischer, M.; Henrich, D.: "Surveillance of Robots using Multiple Colour or Depth Cameras with Distributed Processing", Third ACM/IEEE International Conference on Distributed Smart Cameras (ICDSC 2009), Aug 30 – Sep 02, 2009, Como/Italy.
- [2] S. Gottschalk, M. C. Lin and D. Manocha. OBB-Tree: A Hierarchical Structure for Rapid Interference Detection, Technical report TR96-013, Department of Computer Science, University of N. Carolina, Chapel Hill. Proceedings of ACM Siggraph'96.
- [3] International Federation of Robotics: "World Robotics 2007 - Statistics, Market Analysis, Forecasts, Case Studies and Profitability of Robot Investment", Frankfurt: VDMA Robotik und Automation 2007.
- [4] Kuhn, S.; Henrich, D.: "Multi-View Reconstruction of Unknown Objects in the Presence of Known Occlusions", Technical Report, <http://opus.uni-bayreuth.de/volltexte/2009/576/>, 2009.
- [5] LaValle, S., & Kuffner, J. (2000). RRT-Connect: An Efficient Approach to Single-Query Path Planning. *IEEE Conf. on Robotics and Automation ICRA*.
- [6] Munzert, U.: "Path Planning Algorithms for Remote Laser Welding", Dissertation, TU München 2009
- [7] SMERobot: "The European Robot Initiative for Strengthening the Competitiveness of SMEs in Manufacturing", Integrated Project within the 6th Framework Programme of the EC (March 2005 - May 2009), <http://www.smerobot.org>.
- [8] 3sat broadcast „W wie Wissen“ November 16th, 2008, Title: „Rückschau: Industrieroboter“, [http://www.daserste.de/wiewissen/beitrag\\_dyn~uid.pu4r37ndnjznc665~cm.asp](http://www.daserste.de/wiewissen/beitrag_dyn~uid.pu4r37ndnjznc665~cm.asp)
- [9] William E. Lorensen, Harvey E. Cline: "Marching Cubes: A high resolution 3D surface construction algorithm." In: Computer Graphics, Vol. 21, Nr. 4, Juli 1987, S. 163-169